Available online at www.sciencedirect.com
SCIENCE DIRECT
Precision Engineering 30 (2006) 13–22
PRECISION ENGINEERING
www.elsevier.com/locate/precision

Reliability of parameters of associated base straight line in step height samples: Uncertainty evaluation in step height measurements using nanometrological AFM

Ichiko Misumi [a,*], Satoshi Gonda [a], Tomizo Kurosawa [a], Yasushi Azuma [a], Toshiyuki Fujimoto [a], Isao Kojima [a], Toshihisa Sakurai [b], Tadahiro Ohmi [b], Kiyoshi Takamasu [c]

[a] *National Metrology Institute of Japan, National Institute of Advanced Industrial Science and Technology (NMIJ/AIST), Tsukuba Central 3, 1-1-1 Umezono, Tsukuba, Ibaraki 305-8563, Japan*
[b] *Tohoku University, Aza-Aoba 10, Aramaki, Aoba-ku, Sendai 980-8579, Japan*
[c] *The University of Tokyo, 7-3-1 Hongo, Bunkyo-ku, Tokyo 113-8654, Japan*

Received 13 December 2004; received in revised form 7 March 2005; accepted 16 March 2005
Available online 11 July 2005

Abstract

Step height is widely used as one of the important nanometrological standards for the calibration of nanometrological instruments. In the calculation of step height, a method of determining a base straight line as a reference line is very important. In nanometrology, which is a field of dimensional metrology, an associated feature (Gaussian associated feature), such as a base straight line, is normally calculated from a measured dataset of a metrological instrument on a real feature using the least squares method. The reliability of a base straight line varies depending on the position and number of measured points for the line and the uncertainty in step height calibration also varies depending on the reliability of the base straight line. In this study, we carried the out step height measurement of micropatterned thin films (10, 7, 5, and 3 nm) using an atomic force microscope (AFM) equipped with a three-axis laser interferometer (nanometrological AFM) and evaluated the uncertainty in these measurements. From the uncertainty evaluation results, the uncertainty derived from the reliability of the parameters of the base straight line was one of the major sources of uncertainty when the measured points for the base straight line were varied. An expanded uncertainty ($k = 2$) of less than 0.4 nm was obtained. Furthermore, the reliable range of an associated base straight line in a single step height, such as that in an atomic step sample, was calculated and in importance of the calculation of the reliable range was shown in the uncertainty evaluation and in determining the measurement strategy.

Keywords: Reliability of parameters; Step height; Thickness; Homodyne laser interferometer; AFM; Calibration; Traceability; Nanometrology; Measurement strategy

1. Introduction

Nanometrology, which is dimensional metrology on the nanometer scale, is rapidly gaining importance. In nanometrology, length-standard-traceable measurements are required to certify the values obtained from measurements. National Metrology Institutes (NMIs) have developed length-standard-traceable nanometrological instruments, such as metrological atomic force microscopes (AFMs) [1,2], optical diffractometers (ODs) [3], metrological scanning electron microscopes (SEMs) [4], and interferometrical microscopes (IMs) [5], which satisfy this requirement. The National Metrology Institute of Japan, National Institute of Advanced Industrial Science and Technology (NMIJ/AIST) has developed an AFM equipped with an *XYZ*-axis laser interferometer (nanometrological AFM) and calibrated nanometrological standards with values that are traceable to the unit of length [6]. In the precision measurement of one-dimensional (1D) grating standards (with a nominal pitch of 240 nm) using a

* Corresponding author. Tel.: +81 29 861 4369; fax: +81 29 861 4042.
E-mail address: misumi.i@aist.go.jp (I. Misumi).

0141-6359/$ – see front matter © 2005 Elsevier Inc. All rights reserved.
doi:10.1016/j.precisioneng.2005.03.002

nanometrological AFM, an expanded uncertainty ($k = 2$) of approximately 0.35 nm was obtained [7]. Furthermore, the intercomparison of pitch measurements was performed using an OD, a critical dimension scanning electron microscope (CD-SEM), and a nanometrological AFM, and the consistency of the measurement results was confirmed [7]. As described above, NMIJ/AIST has constructed a calibration system of a 1D grating pitch using a nanometrological AFM.

In nanometrology, not only lateral direction measurements such as 1D grating pitch measurement, but also vertical direction measurements such as step height measurement, are important since the thickness of a thin film is one of the important elements of the International Technology Roadmap for Semiconductors (ITRS) [8]. Stylus instruments (STs), IMs, and metrological AFMs are mainly used in calibrating step height. However, these instruments have different functions. NMIJ/AIST supplies step height calibration services using ST and IM and will soon initiate a service using a nanometrological AFM [9]. From the case of NMIJ/AIST, it is evident that an ST is suitable for relatively large step height samples (step height greater than 500 nm). An IM can carry out noncontact measurements but requires a relatively large step height pattern with a linewidth greater than 30 μm. Our nanometrological AFM is suitable for relatively small step heights (less than 1 μm) and pattern sizes (less than 10 μm). The AFM is a flexible measurement instrument compared with the other two instruments, particularly in the measurements of small step heights, and is occasionally used to calibrate step height samples with various patterns.

For the step height calibration based on ISO 5436-1, the patterns of step height standards are limited to isolated straight lines or grooves and the step height patterns have to be set at the center of the scanning range. Furthermore, the scanning range requires three times the line-width of the pattern to obtain sufficient measured data for the calculation of the associated base straight line. However, the scanning range is insufficient in some cases because of the limitations of the pattern layout in the step height samples, such as atomic steps [10–12]. In the calculation of step height, the manner in which we determine a base straight line as a reference line is crucial. In nanometrology, an associated feature (Gaussian associated feature), such as a base straight line, is normally calculated from a measured data set provided by a metrological instrument on a real feature using the least squares method. The reliability of the base straight line varies depending on the position and number of measured points for this line, and the uncertainty in the step height calibration varies depending on the reliability of the base straight line. In this study, the step height measurement of micropatterned thin films (nominal step height values: 10, 7, 5, and 3 nm) was carried out using a nanometrological AFM, and the uncertainty in step height measurement was evaluated. In the evaluation of the measured uncertainty, the reliability of the parameters of the base straight line obtained using the least squares method is considered as one of the important sources of uncertainty in the measurement.

2. AFM with three-axis laser interferometer (nanometrological AFM)

Fig. 1 shows a photograph of "a nanometrological AFM". Detailed information on the nanometrological AFM is provided elsewhere [1,6]. The nanometrological AFM is a stage scanning-type system, and is operated in the contact

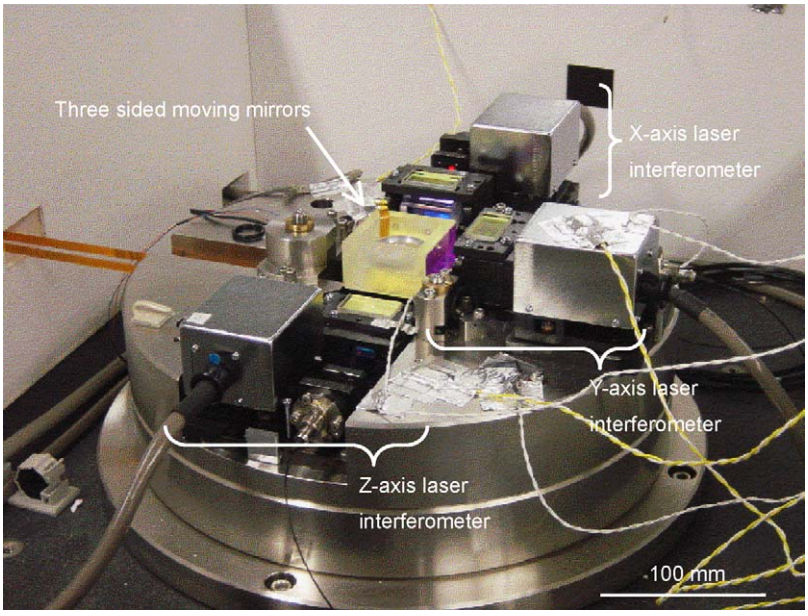

Fig. 1. Atomic force microscope with three-axis laser interferometer (nanometrological AFM). The nanometrological AFM consists of a stage unit, an AFM probe unit, and interferometer units. The probe unit is not mounted in this photograph.

AFM mode. It consists of a stage unit, an AFM probe unit, and interferometer units. The probe unit is not mounted, as shown in Fig. 1. The stage unit comprises a piezo-driven leaf spring stage, which is used as an *XY*-axis scanner, and a tube-type piezoactuator, which is used as a *Z*-axis scanner. The scanning area of this stage unit is approximately 17.5 μm (*X*) × 17.5 μm (*Y*) × 2.5 μm (*Z*). A three-sided moving mirror as the target of the interferometer units is set on top of the *Z*-axis scanner. Each interferometer unit has four optical paths on each axis and its resultant resolution is approximately 0.04 nm. The laser sources of the interferometer unit are practical frequency-stabilized He–Ne lasers with a wavelength of 633 nm (model 117A, Spectra-Physics, Ltd.). The laser frequency is calibrated using an I_2-stabilized He–Ne laser, prior to the step height measurement. The atomic force between a cantilever and a sample surface is detected from the bending of the cantilever using a conventional optical lever method. The *Z*-axis scanner position is servo-controlled so that the atomic force is kept constant during the *XY* scan. The resultant displacement of the *Z*-axis scanner, therefore, corresponds to the displacement of the top of the cantilever at the contact point with the surface. The *XY* scan is servo-controlled using interferometer signals so that the cantilever is positioned to the desired picture element of an AFM image. The *Z*-axis displacement is monitored by the interferometer during the step height measurement. Since the AFM profiles of step height standards are identical to the displacement of the top of the cantilever, the calibration of step height standards is directly traceable to the unit of length.

3. Micropatterned thin film, measurement conditions, and step height calculation

3.1. Micropatterned thin film and measurement conditions

Fig. 2(a) shows a schematic drawing of a micropatterned thin film sample. Thermal oxidized films of silicon substrates were precisely wet-etched using buffered hydrofluoric acid [13]. The thickness of the thin films was checked using the X-ray reflectivity (XRR) [14] method and the etching conditions were optimized. Thereafter, two-dimensional (2D) gratings (with an approximately 3 μm pitch and a 1 μm groove) were fabricated using the thin films. In this study, the nominal step heights of the fabricated gratings, 10, 7, 5, and 3 nm, were defined by the thickness of the thin films obtained by the XRR method before the fabrication. The silicon substrates were approximately 15 mm (*X*) × 15 mm (*Y*). The center of the sample was used for the measurement. The scanning range was approximately 5 μm (*X*) × 5 μm (*Y*) (Fig. 2(b)). Fig. 2(c) shows a schematic drawing of the sectional view of a micropatterned thin film. The step height measurements was performed in a temperature- and humidity-controlled room at 20 °C and 50%, respectively. The nanometrological AFM system was set up on a vibration isolation system and covered with an air turbulence shield to facilitate stable measurements. The surrounding temperature of the sample, ambient temperature, air humidity, and air pressure were recorded during the step height measurements of the micropatterned thin film, and the recorded data were used to compensate for the

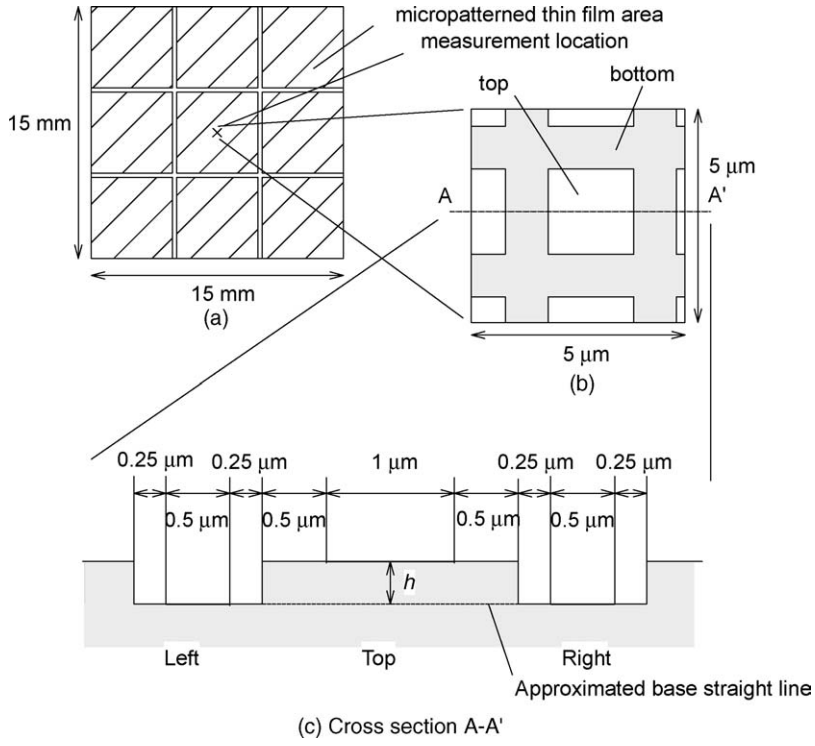

Fig. 2. Schematic drawing of micropatterned thin film samples: (a) entire sample, (b) scanning area, and (c) cross section *A*–*A*′.

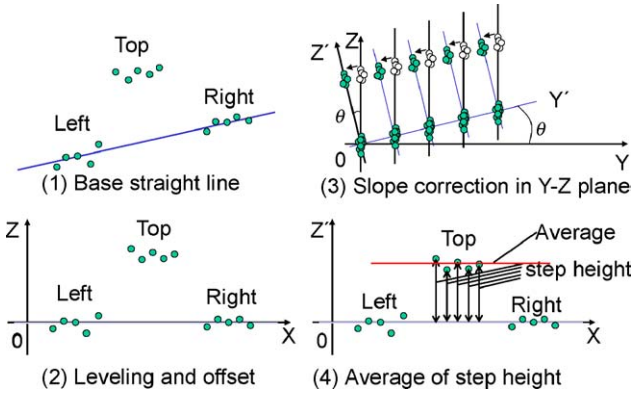

Fig. 3. Procedure for calculation of step height.

refractive index of air [15] and the thermal expansion of the samples [16].

3.2. Step height calculation

Fig. 3 shows the calculation procedure for the determination of the step height of the micropatterned thin films as follows: (1) The slope of a base straight line is calculated by the least square fitting method using the measured data of the left and right parts. (2) Based on the calculated slope of the base line, leveling is carried out and the offset of the slope-corrected line is removed; thus, the base line derived from the left and right parts becomes zero. (3) Following the slope correction in the *X*–*Z* plane, the slope in the *Y*–*Z* plane is also corrected. (4) Step height is calculated as the distance between a point located on the top part and the base line. The average of all step heights is defined as the step height of the line profile.

Fig. 4(a) shows one of the nanometrological AFM images of a micropatterned thin film, prior to slope correction. The scanning direction, scanning speed, scanning range and the number of scanning lines were the *X*-axis, 1 μm/s, 5 μm (*X*) × 5 μm (*Y*) and 128, respectively. Fig. 4(b) shows an example of a line profile for step height calculation. The sampling frequency of the laser interferometer signals in *X*, *Y* and *Z*-axes was approximately 170 Hz and the sampling interval of the laser interferometer signals in the *X*-axis was approximately 6 nm.

4. Uncertainty in step height measurements

4.1. Source of uncertainty

The uncertainty in the step height measurements was evaluated on the basis of "*Guide to the Expression of Uncertainty in Measurement* (*GUM*) [17]" using a method similar to that used for the pitch measurements [6]. Table 1 lists the sources of uncertainty in the step height measurements and pitch measurements [6]. These sources are similar for both the step height and the pitch measurements, except when the uncertainty is derived from the calculation of the base straight line in the step height measurements. The uncertainty derived from the base straight line calculation has one component. A method of evaluating this uncertainty is shown in the next section. Details of the methods for the evaluation of other sources of uncertainty are provided elsewhere [6].

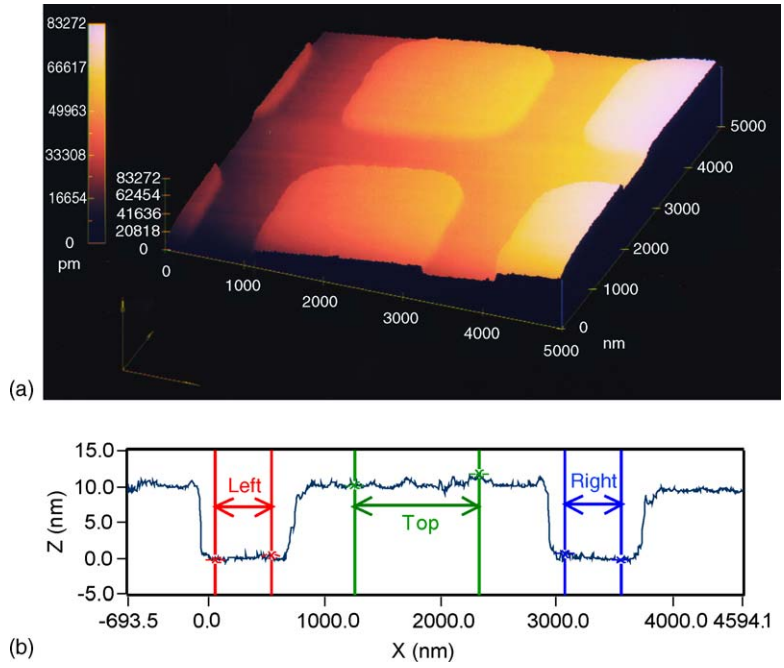

Fig. 4. (a) Nanometrological AFM image of micropatterned thin film (nominal step height: 10 nm; scanning range: 5 μm × 5 μm). (b) Example of line profile for step height calculation. The measured data between the left and right areas are used in calculating the associated base straight line.

Table 1
Sources of uncertainty in step height measurements and pitch measurements of 1D grating (the sources of uncertainty are similar for both step height and pitch measurements, except when the uncertainty is derived from a base line calculation in the step height measurements)

Step height	Pitch
I. Measurement	I. Measurement
(1) Repeatability	(1) Repeatability
(2) Nonuniformity	(2) Nonuniformity
II. Slope correction	II. Slope correction
(1) Cosine error (*X–Z* plane)	(1) Cosine error (*X–Z* plane)
(2) Cosine error (*Y–Z* plane)	(2) Cosine error (*X–Y* plane)
III. Laser interferometer	III. Laser interferometer
(1) Frequency variation of the laser	(1) Frequency variation of the laser
(2) Frequency stability of the laser	(2) Frequency stability of the laser
(3) Change in dead path (temperature)	(3) Change in dead path (temperature)
(4) Change in dead path (thermal expansion)	(4) Change in dead path (thermal expansion)
(5) Interferometer resolution	(5) Interferometer resolution
(6) Cosine error in optical alignment	(6) Cosine error in optical alignment
(7) Abbe error	(7) Abbe error
(8) Change in optical path	(8) Change in optical path
(9) Interferometer nonlinearity (cyclic error)	(9) Interferometer nonlinearity (cyclic error)
IV. Refractive index of air	IV. Refractive index of air
(1) Refractive index of air (temperature)	(1) Refractive index of air (temperature)
(2) Refractive index of air (humidity)	(2) Refractive index of air (humidity)
(3) Refractive index of air (pressure)	(3) Refractive index of air (pressure)
(4) Refractive index of air (CO_2 density)	(4) Refractive index of air (CO_2 density)
V. Sample temperature	V. Sample temperature
(1) Difference in sample temperature	(1) Difference in sample temperature
(2) Thermal expansion	(2) Thermal expansion
VI. Base straight line calculation	
(1) Reliable range of parameters for base	

4.2. Reliability of base straight line parameters

Fig. 5 shows the criterion for the evaluation of step height standards in ISO 5436-1. Three times the line-width is required as the scanning range for this evaluation. However, the micropatterned thin films do not have a sufficient scanning range for the base straight line approximation according to the criterion. Therefore, in the evaluation of measurement uncertainty, the reliability of the parameters for a Gaussian associated base straight line using the least squares method is considered.

The following describes the calculation procedures for the reliable range at any position of the associated feature, $\mathbf{S}_m$ [18–21]. In the following calculations, it is assumed that sectional features have random errors, no correlation, and a normal distribution. The observation Eq. (1), the normal Eq. (2), and the least squares solution (3) have the following relationships:

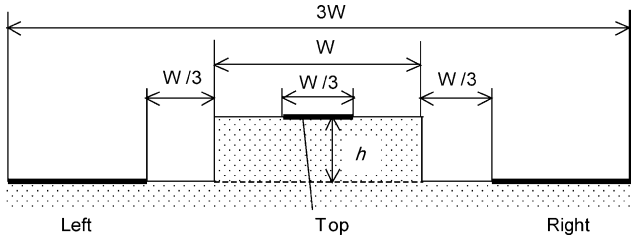

Fig. 5. Schematic representation of criteria for evaluation of step height standards (ISO 5436-1).

$$\mathbf{d} = \mathbf{A}\mathbf{p}, \tag{1}$$

$$\tilde{\mathbf{A}}\mathbf{S}^{-1}\mathbf{A}\mathbf{p} = \tilde{\mathbf{A}}\mathbf{S}^{-1}\mathbf{d}, \tag{2}$$

$$\mathbf{p} = (\tilde{\mathbf{A}}\mathbf{S}^{-1}\mathbf{A})^{-1}\tilde{\mathbf{A}}\mathbf{S}^{-1}\mathbf{d}, \tag{3}$$

where $\mathbf{d}$ is the measured data vector, $\mathbf{A}$ the Jacobian matrix, $\mathbf{p}$ the parameter vector, $\mathbf{S}$ the error matrix of the measured data, and $\tilde{\mathbf{A}}$ is a transposed matrix of $\mathbf{A}$. The error matrix of the parameters $\mathbf{S}_p$ and the error matrix of the calculated values $\mathbf{S}_m$ are obtained, as shown in Eqs. (4) and (5). The diagonal elements of $\mathbf{S}_p$ show the error variances of the parameters, and $\mathbf{S}_m$ shows the variance of the reliable range for a Gaussian associated feature at any point on the associated feature. Eq. (4) describes a transmission from the error of the measured data $\mathbf{S}$ to the errors of parameters $\mathbf{S}_p$, and Eq. (5) describes a transmission from the errors of parameters $\mathbf{S}_p$ to the errors of the calculated values $\mathbf{S}_m$:

$$\mathbf{S}_\mathrm{p} = (\tilde{\mathbf{A}}\mathbf{S}^{-1}\mathbf{A})^{-1} \tag{4}$$

$$\mathbf{S}_\mathrm{m} = \mathbf{A}\mathbf{S}_\mathrm{p}\tilde{\mathbf{A}} \tag{5}$$

If the errors of the measured data $\mathbf{S}$ are known, the error range at any point in the associated feature (the reliable range) $\mathbf{S}_m$ can be calculated using a Jacobian matrix. The Jacobian matrix depends on only the position of the measured points. Therefore, the error of the parameters $\mathbf{S}_p$ can be evaluated

from the position of the measured points and the error of the measured data **S**. The reliability of the calculated results can be evaluated using the least squares method.

From the above equations, the reliable range at any position of the associated feature $\mathbf{S}_m$ can be calculated. The procedure of calculating the reliability in the parameters of the base straight line is as follows. Parameters p_1 and p_2 are determined from y-intercept and the slope. Then, from the observations, Eq. (1) becomes $d = p_1 + p_2 x$. On the basis of the measured points $t_1(x_1, y_1), \ldots, t_n(x_n, y_n)$, the Jacobian matrix **A** of the straight line is expressed as

$$\mathbf{A} = \begin{pmatrix} 1 & x_1 \\ \vdots & \vdots \\ 1 & x_n \end{pmatrix}. \tag{5}$$

Next, the error matrix of the parameters $\mathbf{S}_p$ is obtained. It is assumed that the measured points are positioned in bilateral symmetry with respect to the origin in the area between $x = -0.5D$ and $0.5D$, the measured points have no correlation and the variance in the measured data is σ_0^2. Then, the error matrix of the parameters $\mathbf{S}_p$ is expressed as

$$\mathbf{S}_p = \begin{pmatrix} \sigma_{p1}^2 & 0 \\ 0 & \sigma_{p2}^2 \end{pmatrix} = (\tilde{\mathbf{A}}\mathbf{S}^{-1}\mathbf{A})^{-1} = \sigma_0^2 \begin{pmatrix} \dfrac{1}{n} & 0 \\ 0 & \dfrac{1}{\sum x_i^2} \end{pmatrix}, \tag{6}$$

where n is the number of measured points and x_i is the position of the measured data.

An associated base straight line is located on the X-axis. Therefore, the Jacobian matrix of straight line **A** can be simply expressed as

$$\mathbf{A} = \begin{pmatrix} 1 & x \end{pmatrix}, \tag{7}$$

and the reliable range at any position of the associated base straight line is expressed as

$$\mathbf{S}_m = \sigma_m^2 = \sigma_0^2 \left(\frac{1}{n} + \frac{x^2}{\sum x_i^2} \right). \tag{8}$$

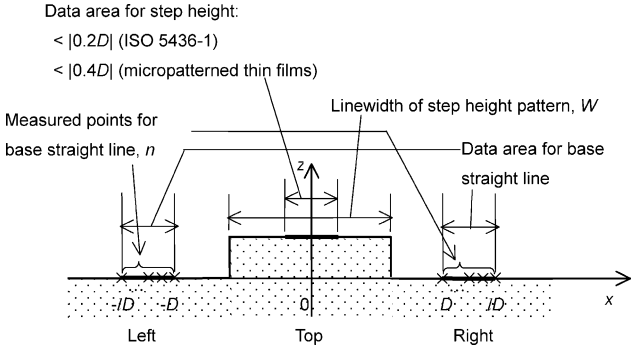

Fig. 6. Measured points for base straight line, n.

The positions of the measured points (number: $2n$) for the base straight line are assumed as shown in Fig. 6. Half of the measured points n are positioned in the area between $x = D$ and lD at even intervals, and the remaining points n are located in the area between $x = -D$ and $-lD$. In this case, the normalized reliable range σ_m/σ_0 is expressed as

$$\frac{\sigma_m}{\sigma_0} = \sqrt{\frac{1}{2n} + \frac{1}{n + (l-1)(n+1) + \frac{1}{6n}(n+1)(2n+1)(l-1)^2} \frac{x^2}{D^2}}. \tag{9}$$

Therefore, we can evaluate the reliable range of a base straight line using Eq. (9).

Fig. 7 shows the relationship between the normalized reliable range σ_m/σ_0 and the normalized horizontal position x/D

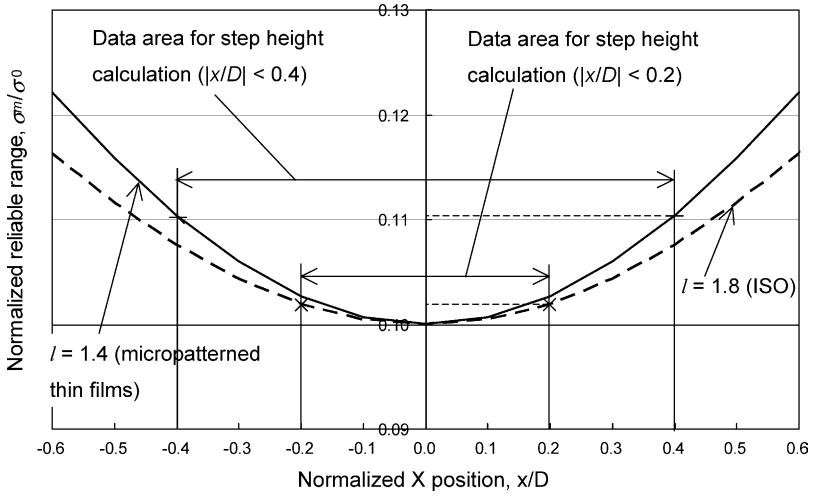

Fig. 7. Normalized reliable range σ_m/σ_0 vs. normalized X position in various areas of measured data for associate base straight line l.

(number of measured points, $2n = 100$). The solid line shows the normalized reliable range in the range of the measured data for the base straight line with $l = 1.4$ (micropatterned thin films), and the dashed line shows the normalized reliable range with $l = 1.8$ (ISO). The normalized reliable range σ_m/σ_0 with $l = 1.4$ is slightly larger than that with $l = 1.8$. The step height of the micropatterned thin films is calculated in the range of $|x/D| < 0.4$. The maximum normalized reliable range σ_m/σ_0 with $l = 1.4$ and $|x/D| < 0.4$ is approximately 0.11. This range is then added to the evaluation of uncertainty in the measurements as an uncertainty component.

5. Measurement results, uncertainty in step height measurements and discussions

5.1. Major sources of uncertainty in step height measurements

Fig. 8 shows six major sources of uncertainty and their standard uncertainties.

5.1.1. Interferometer nonlinearity

The interferometer nonlinearity was the first major source of uncertainty in the step height measurements as well as in the pitch measurements of a 1D grating [6] and the standard uncertainty of interferometer nonlinearity was approximately 0.11 nm. The interferometer nonlinearity caused by residual error in an interpolation process was already reduced by optimizing the correction parameters of the elliptic error in an interference signal. Further adjustment of the optical system and optimization of the correction parameters are needed. A new method of reducing the interferometer nonlinearity is discussed elsewhere [22,23].

5.1.2. Stability of laser frequency

The stability of laser frequency was the second major source of uncertainty in the step height measurements, and the standard uncertainty was approximately 5.2×10^{-2} nm. The standard uncertainty derived from this source $u(f_i)$ was calculated using

$$u(f_i) = \frac{v_{\max}}{f_0} \times \Delta L \times \frac{1}{\sqrt{3}}, \tag{9}$$

where $v_{\max}$ is the maximum Allan variance of the laser frequency taken with various gate times, f_0 the optical frequency of a frequency-stabilized He–Ne laser, and ΔL is an optical path difference between the measurement and reference arms of the laser interferometer. Although an optical arrangement with no optical path difference is a direct means of eliminating the uncertainty $u(f_i)$, such an arrangement tends to require much space in an AFM unit. The use of much stabilized lasers reduces the maximum Allan variance, i.e., uncertainty $u(f_i)$.

5.1.3. Repeatability

The repeatability of the measurements was one of the major sources of uncertainty, and the standard uncertainties approximately ranged from 3.2×10^{-2} to 4.8×10^{-2} nm. It is difficult to decrease the uncertainty derived from this source

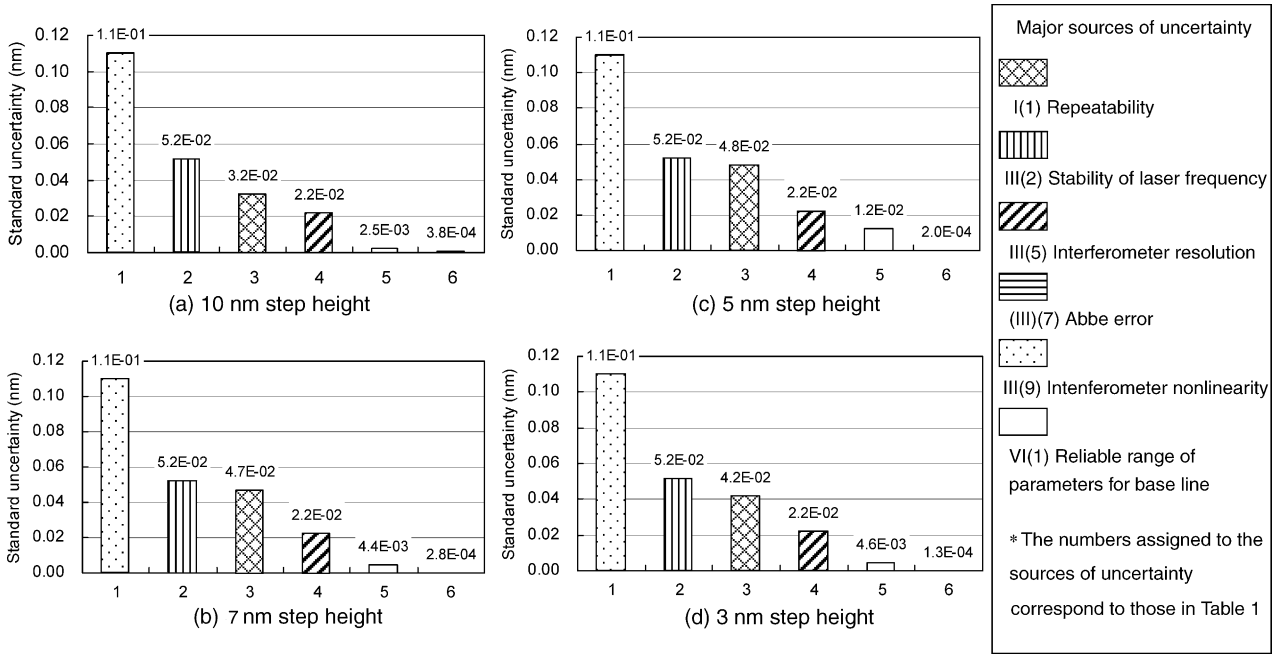

Fig. 8. Major sources of uncertainty and standard uncertainty in step height measurements, where the nominal step heights are (a) 10 nm, (b) 7 nm, (c) 5 nm, and (d) 3 nm.

as there are some factors that still need to be considered, such as stability of probing, positioning accuracy of a scanning stage, setting of the sample and drift in the interferometric measurement.

5.1.4. Interferometer resolution

The resolution of the laser interferometer was another major source of uncertainty, and the standard uncertainty was approximately 2.2×10^{-2} nm. The uncertainty can be decreased theoretically if the number of optical paths or the number of electrical divisions is increased. However, there is some limitation of decreasing the total uncertainty in this case since other uncertainties, for example, the standard uncertainty of interferometer nonlinearity, are greater than the theoretical resolution of the laser interferometer.

5.1.5. Reliable range of parameters for base line

The uncertainty of the reliable range of the parameters was small compared with the other four sources, and the standard uncertainty approximately ranged from 3.0×10^{-3} to 1.6×10^{-2} nm. However, this uncertainty will not be negligible when the measured data variation for the base straight line σ_0 increases, and either the data area for the base straight line will be limited or the standard uncertainties derived from the other major sources will decrease in the future. It is important to plan a measurement strategy in nanometrology, as described in Section 6.

5.1.6. Abbe error

The uncertainty derived from the Abbe error was the sixth major source, and the standard uncertainty approximately ranged from 1.3×10^{-4} to 3.8×10^{-4} nm. The Abbe offset was evaluated as approximately 0.5 mm, and the Abbe error was calculated using it. Detailed information is provided elsewhere [6].

5.2. Measurement results and discussion

Table 2 shows a list of the expanded uncertainties ($k = 2$) and averages of the step heights (nominal step heights: 10, 7, 5, and 3 nm). The expanded uncertainty was approximately 0.27 nm and the order of the uncertainty was same order as to the size of silicon atoms. All average step heights of the samples were larger than the nominal step heights. The offsets are significant considering the expanded uncertainties. The origin of these offsets is unclear; however, some possibilities are considered.

Table 2
Expanded uncertainty U ($k = 2$) and average step height h

Nominal step height (nm)	10	7	5	3
Expanded uncertainty, U ($k = 2$) (nm)	0.26	0.27	0.27	0.27
Average step height, h (nm)	10.5	7.7	5.5	3.6

In this study, the nominal step heights of the fabricated gratings, 10, 7, 5, and 3 nm, were defined by the thickness of the thin films obtained by the XRR method before fabrication. However, it cannot be said that the thickness of the thin films and the step height of the fabricated gratings are exactly the same. This is one of the major reasons for the difference between the nominal step heights and the average step heights.

There are some reasons for the offsets between the measurement results obtained by the AFM and those obtained by the XRR method. The XRR method is one of the most precise measurement tools for determining thin film thickness. However, the XRR method used in this study had no traceability to the length standard or other SI standards, and using this method, it was difficult to get rid of some bias from the obtained results. In general, it is difficult to determine exactly where the interface between a silicon substrate and an oxide film in thickness measurements using the XRR method or ellipsometer. The offsets seem to be caused by the difference between the measurement methods (i.e., AFM versus XRR method).

Furthermore, there were some problems in the sample treatment. Generally, step height standards are covered by some metal film for protection. However, the samples used in this study were not covered by any metal film; hence, their step height might change with time.

6. Discussion: measurement strategy

From the calculations of the normalized reliable range σ_m/σ_0, the number of measured points n was fixed and the area of the measured data for the base straight line l was varied. If l is fixed, σ_m/σ_0 can be obtained for various n. Fig. 9 shows the calculation results of the normalized reliable ranges for various n. When the number of measured points n for the base straight line increases, σ_m/σ_0 decreases. Therefore, the uncertainty of the reliable range for the associated base straight line σ_m/σ_0 also decreases. However, in our nanometrological AFM system, the multiplication of the number of measured points n and the number of scanned lines k is constant, and is approximately 2.2×10^5. If n decreases and k increases, the uncertainty of the repeatability of measurements decreases; however, the uncertainty derived from the reliable range of the parameters σ_m/σ_0 increases. Therefore, there is a trade-off relationship between uncertainty components.

The step height samples used in this study had measurement points for the base straight line on both sides of the step height patterns. In the case of single step height samples, such as the atomic step samples described in the introduction, the reliability of the parameters of a base straight line can be calculated using the same method. The positions of the measured points (number: n) for the base straight line are assumed as shown in Fig. 10(a). It is assumed that all widths of the terraces in the atomic step samples are the same. A base

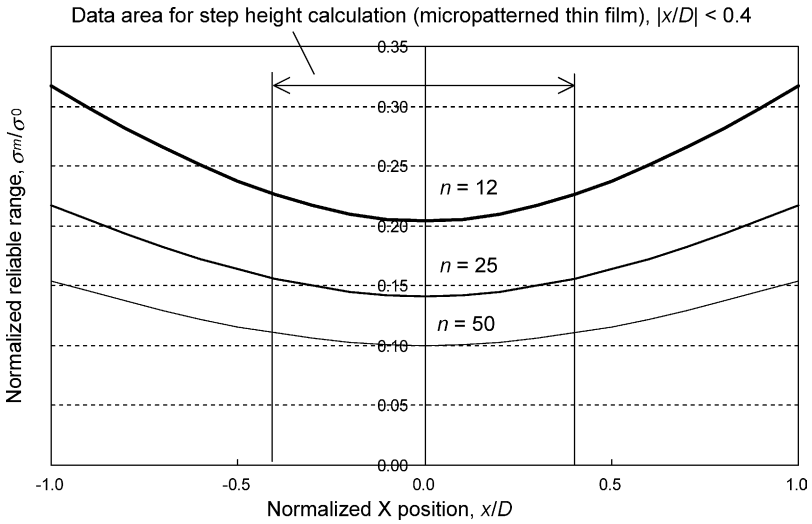

Fig. 9. Normalized reliable range σ_m/σ_0 vs. normalized X position x/D for various numbers of measured data n for associated base straight line.

straight line is calculated from the measured points between $-0.5D$ and $0.5D$. The step height is calculated using the data between $2.5D$ and $3.5D$. The widths of the data area D for the base straight line and the step height calculation are equal to W/3. From Eq. (8) and Fig. 10(a), the normalized reliable range σ_m/σ_0 is expressed as

$$\frac{\sigma_m}{\sigma_0} = \sqrt{\frac{1}{2n} + \frac{12(n-1)}{n(n+1)}\frac{x^2}{D^2}}. \tag{10}$$

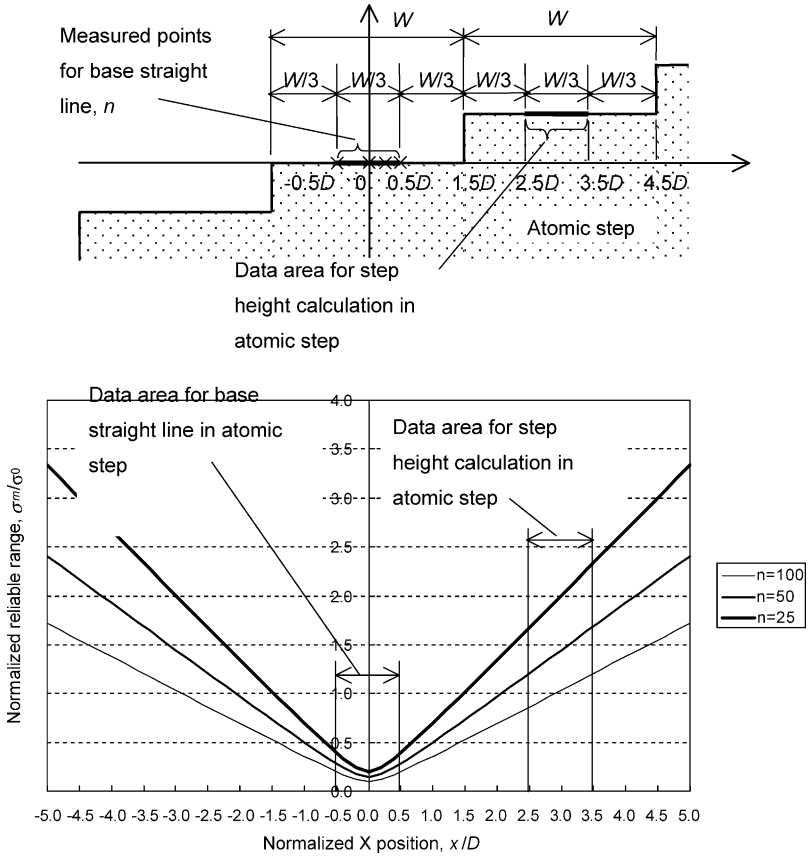

Fig. 10. (a) Schematic drawing of cross section of atomic step sample. W is the width of the terrace in the atomic step sample. It is assumed that a base straight line is calculated from the measured points between $-0.5D$ and $0.5D$. Step height is calculated using the data between $2.5D$ and $3.5D$. The width of the data area D is equal to $W/3$. (b) Normalized reliable range σ_m/σ_0 vs. normalized X position x/D in various areas of the measured data for an associate base straight line. σ_m/σ_0 between $2.5D$ and $3.5D$ is 0.8–2.3.

Fig. 10(b) shows the calculation results of the normalized reliable ranges σ_m/σ_0 for a various measured points n for a base straight line. The normalized reliable range between 2.5D and 3.5D was approximately 0.8–2.3. These values were much greater than those of the normal step height samples shown in Figs. 7–9 since the data area for the step height calculation in one atomic step is not the midpoint of the data areas for the base straight line. The reliable range of the parameters for the base straight line maybecome one of major sources or the first major source of uncertainty.

The measurement conditions can be optimized by calculating the reliable range of the parameters for associated features under the limitations of our measurement instruments. In the uncertainty evaluation results, the first major source of uncertainty was the interferometer nonlinearity. In the near future, if interferometer nonlinearity [22] and the other major sources of uncertainty can be decreased, a measurement strategy involving the calculation of the reliable range for the associated feature, such as the associated base straight line, will gain increasing importance.

7. Conclusions

The step height measurements of micropatterned thin films (with nominal step heights of 10, 7, 5, and 3 nm) were carried out using a nanometrological AFM, and the uncertainty in these measurements was evaluated. The expanded uncertainty ($k = 2$) was less than 0.3 nm. In the evaluation of the uncertainty, the reliability of the parameters of the base straight line was considered as one of the sources of uncertainty. The uncertainty of the reliability of the parameters for the base straight line was the fifth major source of uncertainty among the twenty sources calculated. Furthermore, the calculation method for the reliability of the parameters for the base straight line was applied to the example of a single step height sample, for example, an atomic step sample, and the possibility of the uncertainty of the reliability of the parameters for the base straight line becoming the first major source of uncertainty was shown. The importance of considering the reliability of the parameters for the base straight line was shown, particularly in determining the measurement strategy for the step height measurements of samples with unique shapes.

Acknowledgements

This research was funded in part by the project entitled, “The development of an accurate nanometer roughness measurement method”, No. 00X50023x, Industrial Technology Research Grant Program in 2000 from the New Energy and Industrial Technology Development Organization (NEDO).

References

[1] Gonda S, Doi T, Kurosawa T, Tanimura Y, Hisata N, Yamagishi T, et al. Real-time, interferometrically measuring atomic force microscope for direct calibration of standards. Rev Sci Instrum 1999;70:3362–8.
[2] Gonda S, Doi T, Kurosawa T, Tanimura Y, Hisata N, Yamagishi T, et al. Accurate topographic images using a measuring atomic force microscope. Appl Surf Sci 1999;144–145:505–9.
[3] Meli F, Thalmann R, Blattner P. High precision pitch calibration of gratings using laser diffractometry. In: Proceedings of the 1st International Conference on Precision Engineering and Nanotechnology. 1999. p. 252–5.
[4] Hatsuzawa T, Tanimura Y, Toyoda K, Nara M, Toyonaga S, Hara S, et al. A compact laser interferometer with a piezodriven scanner for metrological measurements in regular SEMs. Rev Sci Instrum 1994;65:2510–3.
[5] Doi T, Kurosawa T. Accurate surface profilometry using interferometric microscope with high magnification. In: Proceedings of the 3rd Euspen International Conference, May 26th–30th. 2002. p. 521–4.
[6] Misumi I, Gonda S, Kurosawa T, Takamasu K. Uncertainty in pitch measurements of one-dimensional grating standards using a nanometrological atomic force microscope. Meas Sci Technol 2003;14:463–71.
[7] Misumi I, Gonda S, Kurosawa T, Tanimura Y, Ochiai N, Kitta J, et al. Submicrometre-pitch intercomparison between optical diffraction, scanning electron microscope and atomic force microscope. Meas Sci Technol 2003;14:2065–74.
[8] ESIA, JEITA, KSIA, TSIA and SIA. International technology roadmap for semiconductors (ITRS); 2004 update.
[9] NMIJ/AIST homepage: http://www.nmij.jp.
[10] Gonda S, Tanaka M, Kurosawa T, Kojima I. Sub-nanometer scale measurements of silicon oxide thickness by spectroscopic ellipsometry. Jpn J Appl Phys 1998;37:L1418–20.
[11] Fu J, Tsai V, Köning R, Dixson R, Vorburger T. Algorithms for calculating single-atom step heights. Nanotechnology 1999;10:428–33.
[12] Dixson R, Orji NG, Fu J, Tsai V, Williams ED, Kacker R, et al. Silicon single atom steps as AFM height standards. In: Proceedings of SPIE 4344. 2001.
[13] Ohmi T, Aoyama S. Calibration of height in atomic force microscope images with subnanometer scale silicon dioxide steps. Appl Phys Lett 1992;61:2479.
[14] Azuma Y. Research on the thin film standard. AIST Bull Metrol 2002;1:475–80 [in Japanese].
[15] Ciddor PE. Refractive index of air: new equations for the visible and near infrared. Appl Opt 1996;35:1566–73.
[16] Okaji M, Imai H. High precision dilatometer by means of optical heterodyne interferometer. Netsu Bussei 1992;6:83–8 [in Japanese].
[17] ISO, BIPM, IEC, IFCC, ISO, IUPAC, IUPAP, and OIML. Guide to the expression of uncertainty in measurement; 1993.
[18] Lotze W. Precision length measurement by computer-aided coordinate measurement. J Phys E: Sci Instrum 1986;19:495.
[19] MacCool J. Systematic and random errors in least squares estimation for circular contours. Prec Eng 1979;1:215.
[20] Takamasu K, Furutani R, Ozono S. Reliability of parameters for associated features in coordinate metrology. J Japan Soc Prec Eng 1997;63:1594–8 [in Japanese].
[21] Takamasu K, Furutani R, Ozono S. Basic concept of feature-based metrology. Measurement 1999;26:151–6.
[22] Keem T, Gonda S, Misumi I, Huang Q, Kurosawa T. Removing nonlinearity of a homodyne interferometer by adjusting the gains of its quadrature detector systems. Appl Opt 2004;43:2443–8.
[23] Keem T, Gonda S, Misumi I, Huang Q, Kurosawa T. Simple, real-time method for removing the cyclic error of a homodyne interferometer with a quadrature detector system. Appl Opt 2005;44:3492–8.